AIAA Propulsion and Energy Forum
19-22 August 2019, Indianapolis, IN
AIAA Propulsion and Energy 2019 Forum

10.2514/6.2019-4220

Combustion of Aluminized Solid Propellants with Bimodal Oxidizer Particle Size Distribution

Bachar Elzein*
Reactions Dynamics, Montréal, Québec, J3B 7B5, Canada

Jacques Xing†
University of Toronto Institute for Aerospace Studies, North York, Ontario, M3H 5T6, Canada

Olivier Jobin‡ and Étienne Robert§
Polytechnique Montréal, Montréal, Québec, H3T 1J4, Canada

The operations and design of solid rocket motors depend heavily of the combustion characteristics of the propellant, mainly the burning rate, the evolution of the burning surface and the propellant's initial geometry. A critical step for the accurate modeling of motor performance starts with the determination of its Vieille's law coefficient a and pressure exponent n. However, the combustion efficiency, for instance as measured through the characteristic velocity C*, should also be known. In this paper, the effects of bimodal ammonium perchlorate (AP) size distribution on propellants burn rate characteristics are experimentally investigated. A series of 12 hot fire tests established a relation between the AP corse to fine (c/f) particles mass fraction and the propellants burning rate, combustion pressure, C* and the mean-mass particle diameter (D_{43}) of aluminum oxide aggregates. The formulations with low AP c/f ratio (smaller average oxidizer particle size) are shown to burn faster and at higher pressures. The estimated mean-mass particle diameter D_{43} of aluminum oxide aggregates is also revealed to increase with decreasing AP c/f mass fraction, possibly due to more intense aerodynamic fragmentation in the burning fuel followed by coagulation of liquid Al_2O_3 droplets in the combustion products. Results show that altering the AP c/f ratio can be used to achieve mission-specific requirements by providing control over the combustion characteristics of solid rocket propellants.

I. Nomenclature

a	=	Vieille's law coefficient
AP	=	ammonium perchlorate
$AP\ c/f$	=	mass ratio of coarse-to-fine AP particles
A_t	=	nozzle throat area, m^2
C^*	=	characteristic velocity, m/s
D_{43}	=	mean-mass particle diameter of aluminum oxide aggregates, μm
D_t	=	throat diameter, m
P_c	=	combustion pressure, Pa
$HTPB$	=	hydroxyl-terminated polybutadiene
k	=	specific heat ratio
$\dot{m}$	=	mass flow, kg/s
n	=	Vieille's law pressure exponent
R	=	gas constant, $J/(kgK)$
$\dot{r}$	=	burn rate, mm/s
ρ_c	=	average density of the continuous phase, kg/m^3
ρ_p	=	average density of the propellant, kg/m^3

*CEO/CTO, 45 Chemin de l'Aéroport, Saint-Jean-sur-Richelieu, QC J3B 7B5
†PhD Candidate, Aerospace Science and Engineering, 4925 Dufferin St, North York, ON M3H 5T6
‡Undergraduate student, Department of Mechanical Engineering, 2900 Boulevard Edouard-Montpetit, Montréal, QC H3T 1J4
§Assistant Professor, Department of Mechanical Engineering, 2900 Boulevard Edouard-Montpetit, Montréal, QC H3T 1J4

T_c = combustion temperature, K
$PBAN$ = polybutadiene acrylonitrile acrylic acid
U_g = gas velocity at distance x, *m/s*
ξ_c = aluminum-oxide concentration, $g \cdot mole/100g$
τ = residence time in the combustor, *ms*

II. Introduction

Modellingof the burning characteristics of propellant formulations is critical in the early design phase of a solid rocket motor, with its burning rate being among the most important parameters. When evaluating a new or modified propellant, its fundamental burning behaviour needs to be obtained experimentally, as analytical frameworks have yet to adequately predict the burning rate based only on chemical ingredients and motor geometry [1]. The most common methods currently available to measure these properties include standard Strand burners (often called Crawford burners), small-scale ballistic evaluation motors and full-scale motors with adequate instrumentation [1, 2]. A Strand burner consists of a small pressure vessel in which a rod-shaped sample of the propellant to be investigated is mounted on a stand. The propellant is ignited and burns from end to end while wires embedded in the sample provide electrical signals as they become exposed to the flame front. Burning rates measured using this approach are typically 4 to 12% lower than the actual values observed in full-size rockets [1]. Although Strand burners do not capture all the complex phenomena taking place in a rocket motor geometry, such as radiative heating and erosive burning, they can still provide useful information on different fuel compositions through simple experiments, but their limitations should be kept in mind when interpreting the results.

Because of safety and cost considerations during testing, rocket motors at reduced sizes have been developed for ballistic evaluation purposes at many research facilities. This is the approach used here to evaluate propellants; such small motors can be fitted with nozzles of different sizes to provide the desired operating pressures. However, the burn rate of a propellant is also known to depend on other variables besides pressure, notably the propellant's chemical formulation, the microstructure of the reactants and the residence time in the combustion chamber.

Propellant formulations incorporating aluminum (Al) particles as the fuel are extensively used, because compared to other metal additives Al has a relatively low cost and has good safety features. The microstructure of the aluminum particles obviously strongly affects the burning behavior and several research groups have investigated this parameter mainly using ammonium perchlorate (AP) as the oxidizer, for a review see the work of Davenas [3]. For instance, DeLuca et al. [4, 5] studied the potential benefits of using nanometric metal particles as fuel and their potential for reducing agglomeration. Jayaraman and Boopathy [6] also evaluated the effects of larger aluminum particle sizes through the comparison of burning rates measured experimentally, using AP/Al in a hydroxyl-terminated polybutadiene (HTPB) binder. Bandera et al. [7] highlighted the existence of a characteristic length based on the spatial displacement of large oxidizer particles, drawing a correlation between the propellants characteristic size, the burning rate and the mean aggregate size at different operating pressures. A bimodal distribution of Al particles (with peaks between 1-3 µm and 15-20 µm) was also shown to help minimize or eliminate unburned aluminum aggregates [8]. These investigations reveal that although the initial aluminum particle size play an important role on aggregate formation, several other parameters are involved and the relationship between them is complex.

A major problem in the combustion of solid rocket propellants is the agglomeration of metal particles, as it impairs energy conversion and can result in a two-phase aerosol flow that reduces specific impulse by 4-6% [7]. Since the combustion efficiency of a solid rocket motor is tributary to its ability to achieve complete combustion of the metal particles contained in the fuel within the motor cavity, a strong correlation exists between the metal oxide aggregate size in the exhaust, the oxidizer microstructure and the propellant burning rate [9, 10].

The present study focuses on the effect of the oxidizer particle geometry on the burning characteristics of solid rocket fuels. AP is the most widely used crystalline oxidizer in solid propellants, because of its good compatibility with various fuels, desirable burning characteristics and availability [1]. To identify the optimal oxidizer particle size for a solid rocket propellant that maximizes combustion efficiency and minimizes the agglomeration of metal oxide particles, different formulations were prepared using a binary mixture of coarse (c) and fine (f) AP particles. All formulations include the same amount of oxidizer and fuel, with the metal additive being exclusively Al particles with a nominal diameter of 3µm. The combustion of Al particles in this size range is well documented in the literature [11–13], with the present study aiming at investigating the effect of the oxidizer particle size on the performance characteristics at low pressure. This Al particle size was also selected because it is easily accessible, has high energy release during the oxidation phase and is easily integrated in the propellant matrix. The bimodal size distribution of AP particles used for

the oxidizer is included with the metal particles in a Polybutadiene Acrylonitrile Acrylic Acid (PBAN) binder, as it leads to easily understood and controllable packing patterns and to desirable plateau burning. The effects of the length of the post-combustion chamber on the combustion efficiency is also investigated. This last parameter is important because the combustion pressures encountered in reduced-scale tests, lower than the 7 MPa typical of large solid motors, requires a post-combustion chamber to achieve the residence times needed for high combustion efficiencies.

III. Experimental Approach

A. Experimental Methods

The combustion behavior of the propellant formulations was captured through the firing of 12 small-scale ballistic evaluation motors featuring a cylindrical perforated grain geometry. A schematic representation of the test stand is shown in Fig. 1. Typically, subscale test motors are used to determine the propellant's burning rate at a certain pressure. Two basic classes of empirical burning rate definitions are in use for motor applications; one is based on propellant thickness and the burning time and is referred to as the thickness/time method, and the second definition is based on the conservation of mass in the motor and is termed mass conservation method.

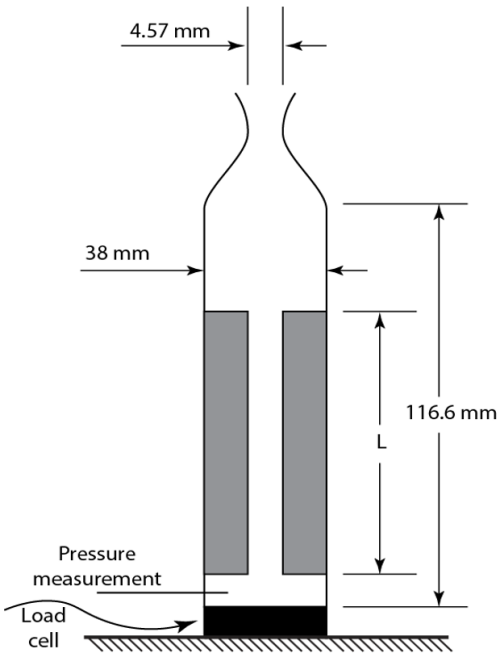

Fig. 1 Schematic representation of the test stand, with *L* as the grain length

For the experiments presented here, the thickness/time method is used. Mass flow rate measurements are carried out using a load cell (TE Connectivity Measurement Specialties, model FC2231-0000-0050-L). Grain web thickness is defined using the averaged measured port diameter after casting and curing. The pressure is measured using a pressure transducer mounted upstream of grain (Measurement Specialties, model MSP-300-2K5-P-3-N-1). The burn time is defined from the pressure trace using the Tangent-Bisector technique [2]. The ratio of the coarse to fine AP particles (AP c/f) is the primary variable under investigation and 4 propellants are evaluated, each containing a different AP c/f mass ratio. To establish a clear baseline for comparison, the fuel and binder proportions are kept identical in the 4 formulations, with the compositions investigated summarized in table 1. The choice of the chemical compositions is based on two criteria: the possibility of benchmarking the experimental results with existing work and consistency with current industrial practice. The former criterion is fulfilled using Dokhan et al. [14] mixture #4 as a reference, corresponding to tests 7 to 9 in the present work. For the latter, the AP size distribution for all formulations features coarse and fine AP particles extensively used in the industry, with a nominal diameter of 400µm and 90µm, respectively.

The propellants are cast in 38mm tubes (33.3 mm I.D) and have a mass loading of 11% binder, 71% ammonium

perchlorate (AP) and 18% 3µm aluminum (Al) particles. The binder used is made of 50% PBAN-Prepolymer, 21.43% Dioctyl Adipate as plasticizer and 28.57% curing agent. The masses of chemical ingredients are measured using an scale with a precision of 10 mg (American Weigh Scales, model AWS-1KG-SIL). Besides the mass ratio of the coarse to fine AP particles (AP c/f) the length of the grain and consequently of the post-combustion chamber is also changed between tests. The post combustion chamber length (L_{P_C}) is defined as the fixed combustion chamber length (L_C) minus the grain length L. Following the procedure described in the next section, these tests are used to determine the Vieille's law coefficient a and the pressure exponent n for each one of the 4 different fuel formulations. The nozzles throat diameter (4.572 mm) was identical for all tests to achieve similar combustion conditions.

Table 1 Compositions of the propellants investigated in the 12 fire tests.

Test #	AP c/f	Al particle size, µm	Grain length (L), mm	Post combustion chamber length (L_{P_c}), mm
1	60/40	3	38.1	78.5
2	60/40	3	50.8	65.8
3	60/40	3	63.5	53.1
4	70/30	3	38.1	78.5
5	70/30	3	50.8	65.8
6	70/30	3	63.5	53.1
7	80/20	3	38.1	78.5
8	80/20	3	50.8	65.8
9	80/20	3	63.5	53.1
10	90/10	3	38.1	78.5
11	90/10	3	50.8	65.8
12	90/10	3	63.5	53.1

B. Experimental Data Analysis

As the reaction progresses during burn rate tests, the mass flow $\dot{m}_c$ exiting the combustion chamber can be modelled by:

$$\dot{m}_c = \rho_f A_b \dot{r} \tag{1}$$

where ρ_f the density of the propellant grain mixture, A_b is the burning area and $\dot{r}$ is the burning rate of the propellant. A simple relationship can be used to correlate the burning rate with the chamber pressure p, Vielle's law:

$$\dot{r} = aP_c^n \tag{2}$$

The Vieille's law coefficient a captures the influence of the grain temperature on the rate of the propellant reaction, while the influence of the pressure is accounted by the exponent n. Another important performance parameter, independent of the nozzle's efficiency, is the characteristic velocity C^*. It is often used to quantify and compare the combustion efficiencies of different propellants at a given temperature and chamber pressure. The characteristic velocity is defined as:

$$C^* = \frac{P_c A_t}{\dot{m}_n} \tag{3}$$

where A_t is the nozzle throat area and $\dot{m}_n$ is the mass flow through it. If the fluid can be considered a perfect gas with a constant specific heat ratio k, equation 3 can be re-written as:

$$C^* = \sqrt{\frac{RT_c}{MW}\frac{1}{k}\left(\frac{k+1}{2}\right)^{\frac{k+1}{k-1}}} \tag{4}$$

Complications arise because the gas constant R, the combustion temperature T_c and the specific heat ratio k are all affected by the combustion pressure P_c. Indeed, gas pressure influences dissociation rates which in turn influence

the composition of the gas in the chamber and hence adiabatic flame temperature, mean molar mass and specific heat ratio. However, the effects can be considered of second order and it is generally reasonable as a first approximation to assume that C^* is approximately constant over the relatively narrow range of combustion pressure considered here. The parameters k, T_c and the mean molecular weight MW are calculated using NASA's Chemical Equilibrium with Applications software [15] for each motor configuration, with averages values of $k = 1.16$, $T_c = 3530.52K$ and $MW = 27.65g/mol$. Under steady state operation, the mass flow generated in the combustion chamber and the mass flow through the nozzle are the same. Of course, this relation does not hold for the transient operations during the pressure build-up and motor tail-off phases. Combining equations 1, 2 and 3 and rearranging yields an expression linking the chamber pressure with C^* and the parameters of Vielles's law:

$$P_c = a\left(C^*\rho_f\frac{A_b}{A_t}\right)^{\frac{1}{1-n}} \tag{5}$$

Assuming a and n constant for a given range of combustion pressures, equation 5 reveals that chamber pressure depends on the geometrical ratio of the burning area A_b divided by the nozzle throat area A_t for a known density ρ_f. It is therefore possible to change the combustion pressure by varying A_b. for instance by changing the grain geometry. As the combustion pressure is measured experimentally, a and n are calculated using a least square method for each of the 4 propellant formulations.

IV. Results and discussion

The burn rate of the propellant was measured for all 12 formulations of table 1 and are shown in Fig. 2 as a function of the AP c/f ratio and of the combustion pressure measured in the chamber. For all post-combustion chamber lengths, propellants with lower AP c/f ratio, i.e with the smaller average oxidizer particle size, are correlated with higher burn rates and higher pressures. The fits of Vieille's law on the experimental data reveal that the pressure exponent is monotonically increasing as the AP c/f ratio is increasing. Generally, one would expect propellant with increased content of ingredients with fine particle sizes to result in both increased burn rates and pressure exponents. However, in the results presented here only the former increase is observed. This is most likely because only the ratio of fine to coarse particles is changed here, with the analysis presented below hinting that this parameter affects combustion efficiency through the coagulation of aluminum particles.

Only one motor was fired for each combination of grain length and AP c/f ratio, and error bars could not be included. From other experimental campaigns realized with motors manufactured with the same process we expect high repeatability (2% variation on the combustion chamber pressure in the firing of 10 identical motors) when the AP c/f ratio is low. When the AP c/f ratio increases, the fuel grain becomes more brittle, increasing the risk that erosion and entrainment at the reacting surface can result in the detachment of fuel fragments. This process, in combination with the limited number of test runs available, might explain why the dataset with an AP c/f composition of 80/20 does not follow this monotonic increase in the pressure exponent. However, this discrepancy does not compromise the general trends observed across all datasets, but should be address in future works involving several firings of identical motors in this composition range resulting in brittle fuel grains.

Experimental results from ref. [14], gathered using a similar propellant formulation as tests # 7-9 from table 1 but covering a broader pressure range, are also plotted for comparison and its burning rate was calculated. Taking into account the similar chemical composition of the propellants used, the results from the current experiment show good agreement with this reference case, with a slight difference in the magnitude of the measured burn rate that can be attributed to a higher average AP particle diameter in ref. [14], as their fine oxidizer was 82.5µm.

The use of propellant grains of different length in a fixed length housing allowed the investigation of the effect of residence time in the post-combustion chamber. The results presented in Fig. 3 reveal that propellants with shorter post-combustion chambers had lower combustion efficiencies, as quantified through the characteristic velocity C*. This trend is likely caused by unburned aluminum remaining in the exhaust, reducing combustion efficiency and hence C* [16], as shown in Fig. 3. In this figure, it is plotted against the time, in ms, spent by the exhaust gases in the post combustion chamber relative to the total residence time in the motor. This figure can also be used to infer the effect of the AP c/f ratio on the characteristic velocity C*, by comparing formulations having the same post-combustion chamber lengths. Although no universal trend is readily identifiable, formulations with higher AP c/f ratios, and hence larger average oxidizer particle sizes, appear to have slightly higher combustion efficiencies, as quantified through C*. The propellant with AP c/f = 90/10 did not exhibit good casting properties and was fragile after curing, accordingly the results from this dataset should be interpreted with care. The test fires of this formulation at L_{P_C} = 78.5 mm and L_{P_C} =

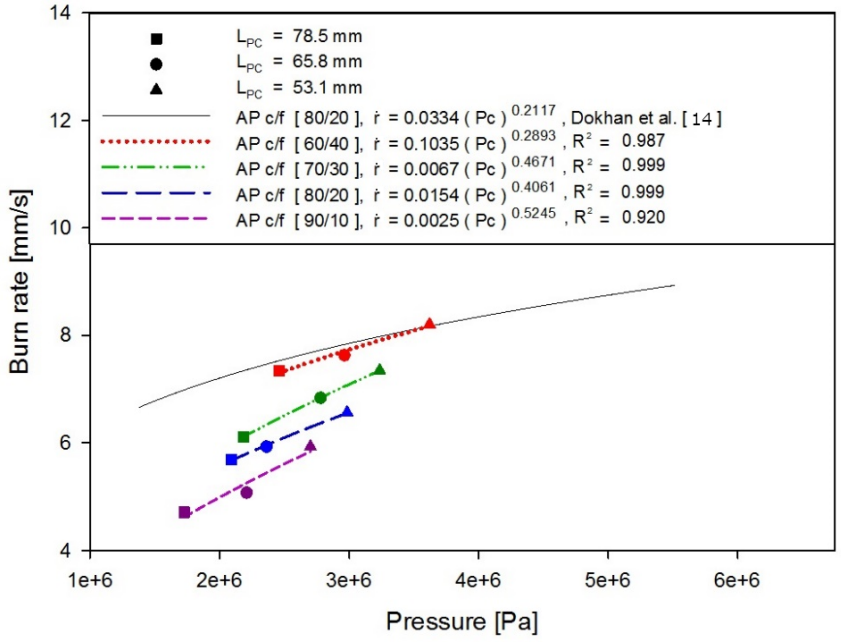

Fig. 2 Burn Rate characteristics of the propellants as function of AP c/f and post combustion chamber length, L_{P_c}.

65.8 mm exhibited pressure spikes in the last phases of their combustion, likely affecting C* in the process, which could justify C* being lower than expected for this dataset.

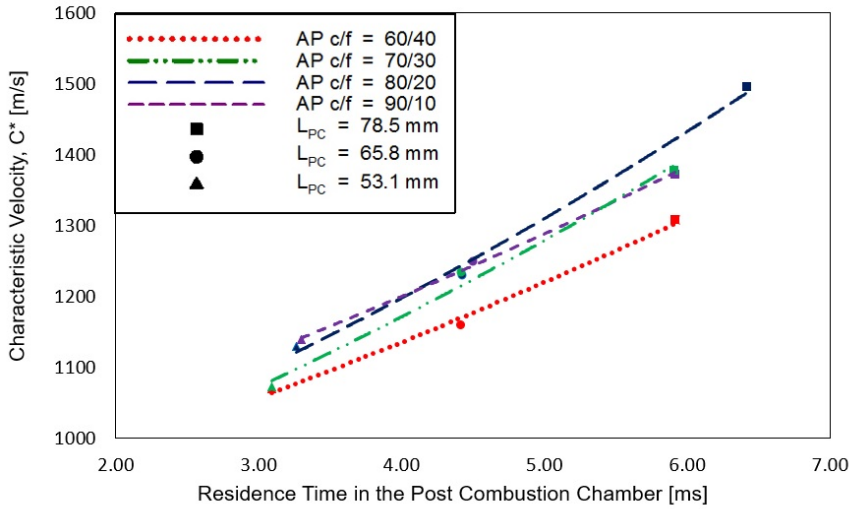

Fig. 3 Characteristic velocity as a function of residence time spent in the post combustion chamber and of the AP c/f ratio. The dashed lines represent least-squares fitted power law functions, R^2 values above 0.97 for all curves.

When considered together, the results presented in Fig. 2 and Fig. 3 reveal that formulations with low AP c/f ratios, i.e. with small average oxidizer particle sizes, have a higher burning rate but a somewhat lower characteristic velocity.

An important parameter controlling this variation appears to be the residence time in the post-combustion chamber. For the results presented in Fig. 3, this time represents between 15% and 55% of the total residence time in the motor, depending mainly on the grain length. To investigate further the difference in performance between propellant having the same AP c/f ratio, the effect of the formation of solid aluminum oxide particles in the exhaust can be considered. Once aluminum oxides are formed in the combustion chamber, solid oxide particles can be formed through condensation and coagulation. In addition to decreasing the amount of gaseous combustion products exiting the motor, and hence the exhaust speed, the presence of such particles induces two-phase flow losses in the nozzle. Largely because of these effects, in solid rocket motors the theoretical specific impulse is not achieved [17]. Such losses can be reduced by decreasing the metal particles ignition time, lowering their initial size or increasing their fragmentation during oxidation, resulting in more complete combustion of the fuel and in the formation of more gaseous products [17].

The size of these aluminum oxide particles can be estimated from fuel composition, motor geometry and the propellant burning characteristics. Because of the importance of these particles on the performance of solid rocket motors, several correlations are available to characterize them [18–27], with the mean-mass particle diameter (D_{43}) typically being the main parameter evaluated. In the following, NASA's CEA software was used to estimate the density of combustion products and the aluminum-oxide concentration downstream of the propellant grain. For this model, the total residence time was defined as the sum of the residence time in the grain and in the post combustion chamber. The former is computed using the relation for the average gas speed upstream of any location x within the fuel grain described in the literature [29] (eq. 6), with x set to the grain length L. The latter is computed using the average velocity in the post-combustion chamber (eq. 7).

$$U_g = \frac{4\rho_p r''}{\rho_c D} x \tag{6}$$

$$U_{P_c} = \frac{\dot{m} x}{\rho_c A} \tag{7}$$

where D is the average grain port diameter during the combustion phase, ρ_c is the average density of the combustion products, ρ_p is the density of the fuel grain and A is the cross-section area of the post combustion chamber. The empirical correlation proposed by Hermsen [27] was used to estimate D_{43}, shown here in metric units:

$$D_{43} = 1.2367 D_t^{0.2932} \left[1 - exp\left(-5.62819258 \xi_c P_c \tau_c\right)\right] \tag{8}$$

where D_t is the throat diameter and P_c is the combustion chamber pressure. ξ_c is the aluminum-oxide concentration and τ_c is the residence time in the combustion chamber.

The results presented in Fig. 4 reveal a clear trend when the residence time in the post-combustion chamber is relatively short. For a given residence time, the formulations with the lowest AP c/f ratios were characterized by a mean oxide particle diameter D_{43} approximately 30% larger that the propellants with the highest AP c/f. Consequently, we can expect reduced gas yields and increased two-phase flow losses in the nozzle when the oxidizer used is finer, explaining the decreased C* computed for such propellant compositions. This is what is observed in Fig. 3, where a low average oxidizer particle size (low AP c/f) is associated lower characteristic velocities, although this effect is relatively small. For all these tests, the initial Al particle size is the same (3μm) and the only difference between formulations is the AP c/f ratio. An explanation for this observation can come from the fact that for low AP c/f propellants the burn rate is higher and hence so is the chamber pressure. This increased pressure increases the condensation rate of aluminum oxide in the post-combustion chamber, increasing the growth rate of oxide particles through particle coagulation, as captured by Hermsen's correlation.

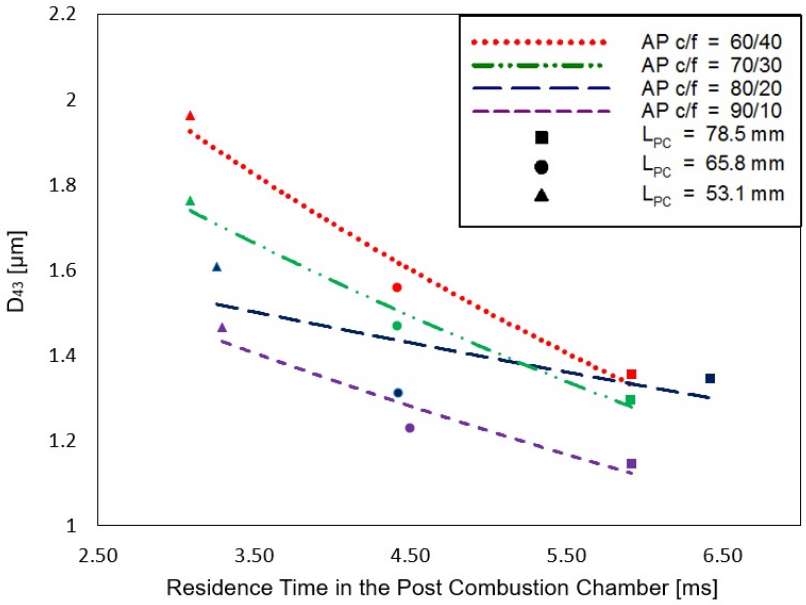

Fig. 4 Mean-mass particle diameter D_{43} as a function of propellant composition, residence time spent in the post combustion chamber and of the AP c/f ratio. The dashed lines represent least-squares fitted power law functions.

V. Conclusion

The impact of the average oxidizer particle size on the combustion of an aluminized composite propellant is investigated using a binary mixture of ammonium perchlorate (AP) particles. The propellant formulations investigated are characterized by the ratio of fine to coarse AP particles (AP c/f), with formulations having a lower AP c/f featuring a higher burn rates but slightly lower characteristic velocities. The impact of the post combustion chamber length on the characteristic velocity, the combustion pressure and the mean-mass particle diameter D_{43} of aluminum oxide aggregates is also evaluated. For all AP c/f ratios, motors with longer post combustion chambers have higher combustion efficiencies, as characterized by the experimentally measured characteristic velocities, correlated with longer residence times for the combustion products in high temperature and high-pressure conditions upstream of the nozzle. The latter observation outlines the limitations of unimodal aluminum particles (3µm nominal diameter) as a fuel for rocket motors operating at pressures between 1.5 and 3.5 MPa as full combustion is not achieved in the propellant grain itself without a post-combustion chamber.

Acknowledgments

The authors wish to express their gratitude to Professor Forman A. Williams from UCSD for his help and valuable advice, Nicholas Montoya for his help regarding logistics as well as to Mark Holthaus, Jerry Irvine, Rick Maschek and John Newman from the FAR testing site at Cantil, California. The authors would like to acknowledge the logistical support of Kim Gallagher at Aerotech for assistance with ammonium perchlorate shipping and handling, as well as André Choquette for his assistance regarding experimental measurements.

References

[1] Sutton, G., and Biblarz, O., *Rocket Propulsion Elements*, 7th ed., Wiley-Interscience, New York, 2001, Chap. 11, p. 751.

[2] Schulz, R. J., *A Short Course on Fundamentals of Solid Rocket Motors*, The University of Tennessee Space Institute, Tullahoma, Tennessee, 1991.

[3] Davenas, A., "Development of Modern Solid Propellants," *Journal of Propulsion and Power*, Vol. 19, No. 6, 2003, pp. 1108–1128. doi:10.2514/2.6947.

[4] DeLuca, L. T., "Burning of Aluminized Solid Rocket Propellants: from Micrometric to Nanometric Fuel Size," *International Autumn Seminar on Propellants, Explosives and Pyrotechnics (IASPEP)*, Vol. 7, 2007, pp. 277–289. doi:10.2514/2.6947.

[5] DeLuca, L. T., Galfetti, L., Sverini, F., Meda, L., Marra, G., Vorozhtsow, A. B., Sedoi, V., and Babuk, V., "Burning of Nano-Aluminized Composite Rocket Propellants," *Combustion, Explosion and Shock Waves*, Vol. 41, No. 6, 2005, pp. 680–692. doi:10.1007/s10573-005-0080-5.

[6] Jayaraman, K., and Boopathy, G., "Aluminum Agglomerate Size Measurements in Composite Propellant Combustion," *Innovative Design and Development Practices in Aerospace and Automotive Engineering*, Lecture Notes in Mechanical Engineering, Springer, 2017, pp. 437–445. doi:10.1007/978-981-10-1771-1_47.

[7] DeLuca, L., Bandera, A., and Maggi, F., "Agglomeration of Aluminized Solid Rocket Propellants," *45th AIAA/ASME/SAE/ASEE Joint Propulsion Conference & Exhibit*, 2009. doi:10.2514/6.2009-5439.

[8] Geisler, R., "A Global View of the Use of Aluminum Fuel in Solid Rocket Motors," *38th AIAA/ASME/SAE/ASEE Joint Propulsion Conference & Exhibit*, 2002. doi:10.2514/6.2002-3748.

[9] Willoughby, P., Baker, K., and Hermsen, R., "Photographic Study of Solid Propellants Burning in an Acceleration Environment," *Symposium (International) on Combustion*, Vol. 13, No. 1, 1971, pp. 1033 – 1045. doi:10.1016/S0082-0784(71)80102-9.

[10] Hermsen, R., "Aluminum Combustion Efficiency in Solid Rocket Motors," *19th Aerospace Sciences Meeting*, 1981. doi:10.2514/6.1981-38.

[11] Bojko, B. T., DesJardin, P. E., and Washburn, E. B., "On modeling the diffusion to kinetically controlled burning limits of micron-sized aluminum particles," *Combustion and Flame*, Vol. 161, No. 12, 2014, pp. 3211 – 3221. doi:10.1016/j.combustflame.2014.06.011.

[12] Bazyn, T., Krier, H., and Glumac, N., "Evidence for the transition from the diffusion-limit in aluminum particle combustion," *Proceedings of the Combustion Institute*, Vol. 31 II, 2007, pp. 2021–2028. doi:10.1016/j.proci.2006.07.161.

[13] Zaseck, C. R., Son, S. F., and Pourpoint, T. L., "Combustion of micron-aluminum and hydrogen peroxide propellants," *Combustion and Flame*, Vol. 160, No. 1, 2013, pp. 184 – 190. doi:10.1016/j.combustflame.2012.10.001.

[14] Dokhan, A., Price, E., Sigman, R., and Seitzman, J., "The effects of Al particle size on the burning rate and residual oxide in aluminized propellants," *37th Joint Propulsion Conference and Exhibit*, 2001. doi:10.2514/6.2001-3581.

[15] McBride, B. J., and Gordon, S., "Computer Program for Calculating and fitting Thermodynamic Functions," *NASA RP-1271*, 1992.

[16] Cheung, H., and Cohen, N. S., "Performance of solid propellants containing metal additives," *AIAA Journal*, Vol. 3, No. 2, 1965, pp. 250–257. doi:10.2514/3.2838.

[17] Sippel, T. R., Son, S. F., and Groven, L. J., "Aluminum agglomeration reduction in a composite propellant using tailored Al/PTFE particles," *Combustion and Flame*, Vol. 161, No. 1, 2014, pp. 311 – 321. doi:10.1016/j.combustflame.2013.08.009.

[18] Fein, H. L., "A Theoretical Model for Predicting Aluminum Oxide Particle Size Distributions in Rocket Exhausts," *AIAA Journal*, Vol. 4, No. 1, 1966, pp. 92–98. doi:10.2514/3.3389.

[19] Hoglund, R., and Jenkins, R., "A unified theory of particle growth in rocket chambers and nozzles," *5th Propulsion Joint Specialist*, 1969. doi:10.2514/6.1969-541.

[20] Golovin, A. M., "On the Kinetic Equation for Coagulating Cloud Droplets with Allowance for Condensation," *Geophysics Series*, Vol. 10, 1963, pp. 949–953.

[21] Marble, F. E., "Droplet Agglomeration in Rocket Nozzles Caused by Particle Slip and Collision," *Astronautica Acta*, Vol. 12, No. 2, 1967, pp. 159–166.

[22] Nack, T. H., "Theory of Particle Agglomeration, Mean Size Determination and Chamber Coagulation in Rocket Motors," *Proceedings of the AFRPL Two-Phase Flow Conference*, Vol. I, 1967, p. 103.

[23] Crowe, C. T., and Willoughby, P. G., "A study of particle growth in a rocket nozzle," *AIAA Journal*, Vol. 5, No. 7, 1967, pp. 1300–1304. doi:10.2514/3.4187.

[24] Davanlou, A., Lee, J. D., Basu, S., and Kumar, R., "Effect of viscosity and surface tension on breakup and coalescence of bicomponent sprays," *Chemical Engineering Science*, Vol. 131, 2015, pp. 243 – 255. doi:10.1016/j.ces.2015.03.057.

[25] Kurzius, S. C., and Raabr, F. H., "Measurement of Droplet Sizes in Liquid Jets Atomized in Low Density Supersonic Streams," *NASA CR-1242*, 1968, p. 2.

[26] Kovalev, O. B., "Motor and Plume Particle Size Prediction in Solid-Propellant Rocket Motors," *Journal of Propulsion and Power*, Vol. 18, No. 6, 2002, pp. 1199–1210. doi:10.2514/2.6079.

[27] Hermsen, R., "Aluminum Oxide Particle Size for Solid Rocket Motor Performance Prediction," *Journal of Spacecraft and Rockets*, Vol. 18, No. 6, 1981, pp. 483–490. doi:10.2514/3.57845.